J. Flow Injection Anal., Vol. 32, No. 2 (2015) 81–87

Recent Development in the Fundamental Functions of Compact Disc-type Microfluidic Platform

Shuai Guo, and Toshihiko Imato

Department of Applied Chemistry, Graduate School of Engineering, Kyushu University, Fukuoka, 819-0395, Japan

Abstract

Compact disc (CD)-type or centrifugal microfluidic platforms gain more and more attentions from the researchers in last few years (2012-2015). Various works and designs of the unit operations on the CD-type microfluidic platforms have been proposed to satisfy the requirements for the applications in wide fields such as biochemical analysis and diagnostics. In this review, we introduce the recent development in the fundamental functions of the CD-type microfluidic platform in the period of 2012-2015, such as valving, mixing, separation and the adjustment of flow sequencing.

Keywords CD-type microfluidic platform, centrifugal microfluidics, pumping, valving, mixing, separation, flow sequencing

1. Introduction

Since the first development of the compact disc (CD)-type or centrifugal microfluidic platform was investigated in last decades [1-5], this kind of device has already been recognized as one of a powerful tool in the analytical sciences. The necessary laboratorial microfluidic functions such as sample injection, separation, mixing, reaction and detection have already been successfully fabricated on the CD-sized device, which allows the automation and integration of the complex assay protocols in the analytical chemistry. The CD-type microfluidic platform gains more and more attentions from the researchers in last few years (2012-2015), both in the development of the fundamental functions and applications in biochemical analysis.

In this review, we introduce the recent progress in the fundamental functions on the CD-type microfluidic platform, such as valving, mixing, separation and adjustment of flow sequencing from 2012 to 2015.

2. Valving

The CD-type microfluidic platform usually uses the centrifugal force as the driving force by rotating the device on a turn-table, and the value of the centrifugal force can be adjusted by changing the rotation speed, as well as the location of the solution reservoir and the geometry of the microchannel. On the contrast, in order to adjust the flow sequencing of the solutions on the device, various valving methods have been developed in last decades [5-11] to cooperate with the centrifugal force to carry out the analytical applications, from passive valves to active valves. To satisfy the requirements in analytical applications, the researchers made large progress in designing various valving units in the last few years [12-32]. Z. Cai *et al.* [15-16] proposed a magnetically actuated valve by using the external magnetic field as well as the additional mechanical components. L. X. Kong *et al.* [21] developed a passive valve using the wax. Y. Kim *et al.* [24] used the so-called solvent-tolerable valve to control the microfluidic flow by the assistance of the laser irradiation, and M.-S. Choi *et al.* [26] also developed a laser-burst valve by using the laser beam to control the open and close of the valve. Furthermore, T. Kawai *et al.* [30] designed a so-called rotatable reagent cartridge structure as the valve to control the flow of 4 different solutions.

A. Kazemzadeh *et al.* [12] designed a simple passive gate valve for the purpose of switching the flow direction of the solution out of the microchannel. As shown in Fig. 1, compared with the conventional capillary valve at the T-junction, the authors designed a gate valve with the special geometrical structures at the T-shaped junctions. According to the simulation results from the authors, the fluid meniscus has a concave shape due to the hydrophilic surface of the microchannel in both conventional valve and gate valve when the flowing time is earlier than 0.1 s. However, after the flowing time of 0.8 s, the liquid motion in the gate valve is different compared with the conventional valve.

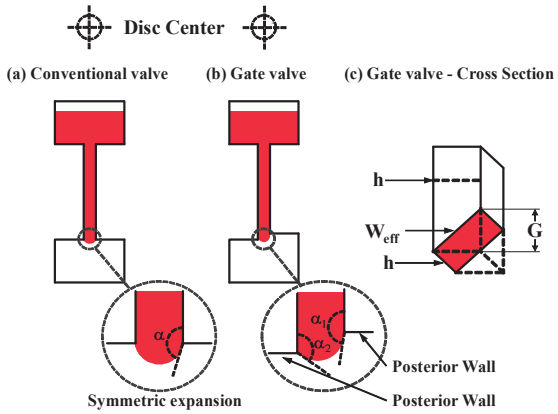

Fig. 1 A sketch of (a) a conventional capillary valve, (b) a gate valve and (c) the cross section of a gate valve [12].

The switching of the flow direction of the solution was realized by applying both the components of the geometrical effect at the T-shaped junction as well as the Coriolis force, according to the authors. When the device was rotating at a low frequency, the solution flowed in the opposite direction of the Coriolis force, and when the rotation frequency was increased to a high value, the flow direction of the solution was switched to the direction of the Coriolis force. The crucial advantage of the authors' design is that there is no need to neither change the direction of the rotation nor apply external forces to switch the

flow direction of the solution, which allows for multiplexed and more sophisticated assays on the centrifugal microfluidic platforms without interrupting other operations. The effect of gating parameter *G* on flow behavior and burst frequency in the CD-type microfluidic platform has been studied experimentally and numerically by the authors. The results show that the gate valve can change the flow direction when the gating parameter *G* is approximately half of the capillary width (0.4-0.5 width).

L. Swayne *et al.* [13] developed a rapid prototyping of pneumatically actuated hydrocarbon gel valve on the CD-type microfluidic platform. As shown in Fig. 2, a 4 mm length of commercially available petroleum jelly was located inside an 800 μm deep channel (Fig. 2 e) and positioned to block flow out of a 100 μm deep channel (Fig. 2 c) connected to an 800 μm deep liquid reservoir (Fig. 2 b). The plug was slightly thicker than the channel from which liquid flows while only partially covering the channel in which it resides.

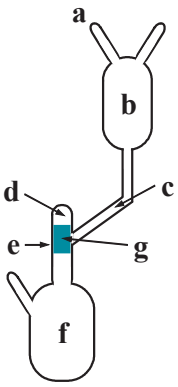

Fig. 2 Design of a single unit of the CD-type microfluidic platform. Each device contains 6 units with (a) injection and vent ports, (b) liquid reservoir, (c) 100 μm deep channel cut in the bottom adhesive layer, (d) 800 μm deep channel with air inlet at top, (e) petroleum jelly plug, (f) receiving chamber, and (g) expanded view of junction of plug highlighting the critical difference in channel depth and plug height [13].

According to the authors, without using the petroleum jelly plug in the 800 μm deep channel, the solution was found to flow through the open 100 μm deep channel at a rotation frequency of 300 rpm. With the plug in place, the maximum leak-free rotation frequency achieved was 1300 rpm for 10 s of rotation. When using the air stream to open the plug, the solution was immediately flowed into the receiving reservoir. This inexpensive, easy to fabricate, active hydrocarbon gel-based valve on the CD-type microfluidic platform does not involve complex preparation or time-consuming installation methods, which permits it to be implemented in manufactured end products. Additionally, the valve can be used in conjunction with passive capillary valves to eliminate the need for consecutively smaller valves and higher burst frequencies.

W. Al-Faqheri *et al.* [14] developed an interesting passive check valve cooperating with a thermo-pneumatic pumping on the CD-type microfluidic platform. As shown in Fig. 3, a terminal check valve (TCV) that restricts air flow in one direction between the microfluidic process and the surrounding environment, and a bridge check valve (BCV) that allows one way flow of air and liquid between two points in the microfluidic process were developed by the authors. Fig. 3 (a1-a3) illustrates the operation of the TCV. When positive air pressure is applied to the inlet of the TCV, the latex is deflected upwards towards the open space between the top and bottom covers. Air can then travel through the space created by the deflection, and then via the air exchange hole to escape through the outlet (Fig. 3 a2). However, when a negative pressure is applied on the inlet, thus forming an air tight seal, an air flow through the valve is restricted (Fig. 3 a3). In this configuration, the TCV chip can be installed on the CD with the inlet facing the CD surface to allow only one way air flow from within the CD to the surrounding environment. By flipping the TCV chip over, and having the top cover placed on the CD-surface, it will then allow only one way air flow from the surrounding environment into the CD (Fig. 3 b1-b3).

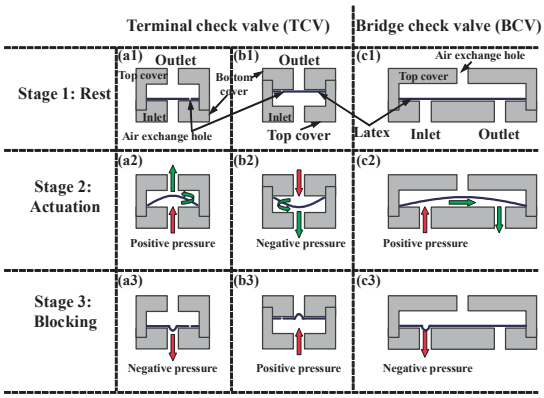

Fig. 3 Check valve operation principle. (a1, b1 and c1) TCV and BCV valve at rest, (a2) TCV valve activated by applying positive pressure at the inlet, (b2) TCV valve activated by implementing negative pressure at the inlet, (c2) BCV valve activated by applying positive pressure at the inlet, (a3) TCV valve blocking air-flow due to the negative pressure at the inlet, (b3) TCV valve blocking air-flow by implementing positive pressure at the inlet, (c3) BCV valve blocking air/liquid flow as negative pressure is applied at the inlet [14].

Fig. 3 (c1-c3) demonstrates the principle of operation for the BCV. As both the inlet and outlets are in the bottom cover in this case, it tis the bottom cover that must be placed on the CD surface. When the CD is at rest, the latex film is flat against the bottom layer (Fig. 3 c1). When a positive pressure is applied on the inlet of the BCV valve, the latex film is deflected upwards, and air/liquid is allowed to flow through the space under the latex to the outlet (Fig. 3 c2). However, when a negative pressure is applied on the inlet of the BCV valve, the latex forms a tight seal on the bottom layer, preventing any backwards flow of air/liquid (Fig. 3 c3).

As shown in Fig. 4, by cooperating with the thermos-pneumatic pumping (TPP) reservoir, the flow process can be adjusted accurately. By heating the TPP reservoir to generate a positive air pressure, the TCV valve is blocking and the BCV chip is activated, so that the red solution is flowed through the BCV chip into the waste reservoir (Fig. 4 b). Then by cooling down the TPP reservoir to room temperature, the generated negative pressure makes the TCV valve to be

activated, and the BCV chip to be blocking, so that the blue solution is flowed into the intermediate reservoir A (Fig. 4 c). After a rest step (Fig. 4 d), heat the TPP reservoir again to generate the positive air pressure, the TCV valve is blocking and no air flow is allowed through the surrounding environment. On the other hand, the BCV chip is activated, and the positive air pressure push the blue solution to flow through the BCV chip into the waste reservoir (Fig. 4 e) to mix with the red solution located previously (Fig. 4 f).

The experimental results of the liquid swapping process show that the developed TCV and BCV are able to accurately control the direction of the air/liquid flow. In an extended example, the authors performed ELISA assay for Dengue fever detection on the device. The proposed design presents a fully automated ELISA process with full isolation from the environment to prevent contamination of the samples and reagents.

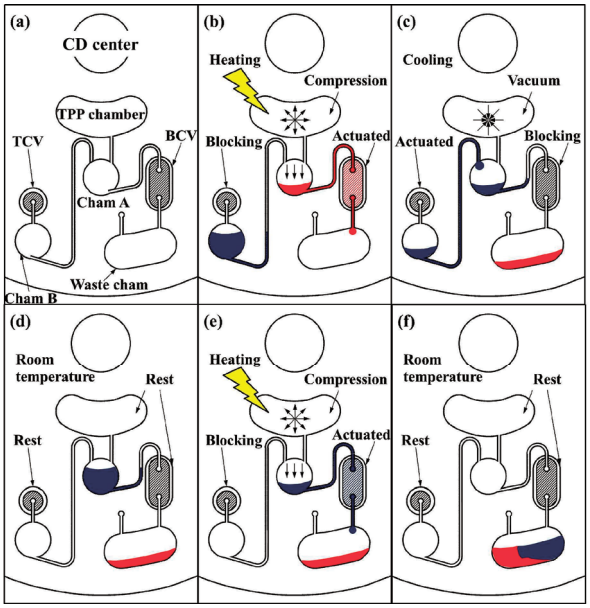

Fig. 4 Liquid swapping sequence, (a) liquid status before start the process, (b) heating the TPP chamber where the TCV valve is blocked while the BCV chip is activated, (c) cooling the TPP chamber actuates pull pumping where the TCV valve is activated and the BCV chip is blocking reverse airflow from the waste chamber, (d) liquid position after the cooling process stops, (e) heating the TPP chamber pushes the liquid from chamber A towards the waste chamber, (f) final liquid status [14].

3. Mixing

It is always a problem to achieve fast mixing on the CD-type microfluidic platform, which is important and essential for applying in bioanalytical applications. The microscale flow is strictly laminar, which makes the mixing largely determined by the free diffusion of the molecules, unlike the large-scale convection motion in the test tube. However, the molecular diffusion coefficient is typically very small for the large macromolecules (i.e. protein), which is about 10^{-11} m^2/s. In assuming the cross-sectional dimension of the microchannel is 100 μm, the time scale for macromolecule diffusion is about 17 min [33]. In order to increase the mixing speed, additional force to generate the chaotic advection by actuation of paramagnetic beads in an external field [34-37] has been proposed by the researchers. However, these kinds of active mixers require some external moving parts, and sometimes complicated in preparation and inconvenient to cooperate with other microfluidic components. In last few years, the researchers tend to develop passive mixers to achieve the fast mixing speed on the CD-type microfluidic platform, by introducing crossflow in the microchannel [38-41].

Y. Ren *et al.* [38] discussed about the role of zigzag microchannel in increasing the mixing efficiency on the CD-type microfluidic platform both numerically and experimentally. As shown in Fig. 5, the authors compared the mixing efficiency in the zigzag microchannel and in the radial straightforward channel.

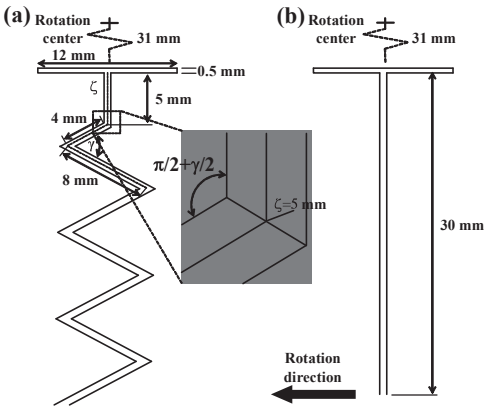

Fig. 5 Schematic of two models: (a) zigzag channel; (b) radial channel [38].

The authors classified that there are three kinds of accelerations acting on the liquid in the zigzag channel, the Coriolis acceleration a_{cor}, the crossflow acceleration a_s and the local centrifugal acceleration a_b due to the channel bend. When the channel segment in the zigzag channel is inclined towards the rotation direction (prograde), all three accelerations are aligned intensifying the cross flow. However, when the channel segment in the zigzag channel is inclined opposite to rotation direction (retrograde), the Coriolis acceleration competes with the other two accelerations producing complex flow. Comparing with the performance of mixing in the radial microchannel, the mixing in the zigzag channel still benefits so much due to the cross-section flow accelerated by the centrifugal acceleration and the bend acceleration. Both the simulation and the experimental results reveal that overall mixing quality for rotating zigzag channel is much improved compared to rotating radial channel at same rotation speed.

J.-N. Kuo *et al.* [39] improved the study in mixing from zigzag channel to the square-wave channel, and made optimization in the square-wave channel design to improve the performance of mixing. As Fig. 6 shows, the authors compared the mixing efficiencies in three kinds of microchannels, the square-wave one, the curved one and the zigzag one. As the device rotates, three different body forces are generated within the microchannel, namely a centrifugal force f_w due to the system rotation, a Coriolis force f_C due to the combined effects of the system rotation and the liquid velocity, and a centrifugal force f_R generated by the microchannel curvature. According to the authors, the simulation results show that the mixing index at

the outlet of the three microchannels gave different values of the rotation speed. For all three microchannels, the mixing index reduces with an increasing rotation speed due to the shorter residence time that arises from the rotation at high speed. For a given rotation speed, the square-wave microchannel achieves the best mixing performance longer flow path results in a longer retention time and a strong chaotic stirring occurs as a result of eddies at the bends in the microchannel.

The authors also optimized the geometry of the square-wave microchannel to achieve a good mixing performance. They designed four different square-wave microchannels with different width and length in the x- and y-axis direction in the square-wave stages. The results show that the 100 μm width of microchannel in stage 1 and 3 with the 300 μm width of microchannel in stage 2 achieves the best mixing performance, which is also proved by the experimental results in mixing the plasma with the DI water.

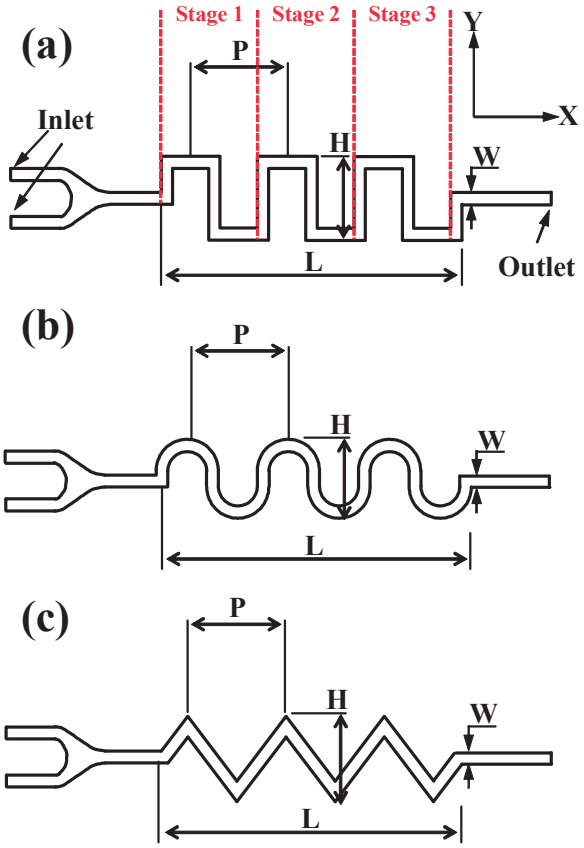

Fig. 6 Schematic illustrations of (a) square-wave microchannel, (b) curved microchannel and (c) zig-zag microchannel [39].

4. Separation

In order to widely spread the applications of CD-type microfluidic platform in the clinical diagnostic procedures, the blood test must be successfully carried out on the device. The first step in performing a blood test is generally to separate the blood plasma (or cell-free serum) from the whole human blood so as to remove the blood cells and cellular components [42], which may otherwise confuses the analysis results [43]. Traditionally the separation process is performed in a laboratory using bench-top centrifugation equipment, which is expensive, labor intensive and time-consuming, and cannot meet the requirement of point-of-care (POC) applications, which urges rapid, straightforward and low-cost automated systems capable of performing the complete plasma separation and preparation process in a more seamless and efficient manner. In last few years, the separation of human whole blood on the CD-type microfluidic platform by using the centrifugal force generated from the rotation has been largely developed, and many researchers proposed different methods to realize the separation process as well as improve the separation performance [46-59]. T. Morijiri *et al.* [49] presented a microfluidic counterflow centrifugal elutriation (CCE) system for sedimentation-based cell separation. E. J. Templeton *et al.* [53] worked on another direction, by sealing the commercially available filter paper into the centrifugal microfluidic device to realize the separation unit. D. Kirby *et al.* [57] applied the external magnetic field to develop a centrifugo-magnetophoretic purification system to separate the rare cancer cells from the human blood. And D. J. Kinahan *et al.* [59] designed a *spira mirabilis* (equiangular spiral) structure under the identified geometric conditions to enhance the separation performance by increasing the Boycott effect.

J.-N. Kuo *et al.* [46] developed a simple CD-type microfluidic platform in which the plasma is first separated from the whole human blood, then divided into two samples of equal volume, and finally decanted into a detection reservoir for analysis purposes. As show in Fig. 7, the microchannel network comprises a plasma separation network and a splitter/decantation network. The plasma separation network consists of a straight microchannel, a curved microchannel and a branched microchannel. As the device rotates, the blood within the separation network is subjected to three different body forces, namely a centrifugal force f_W due to the system rotation, a Coriolis force f_C due to the combined effects of the system rotation and the liquid velocity, and a centrifugal force f_R generated by the microchannel curvature.

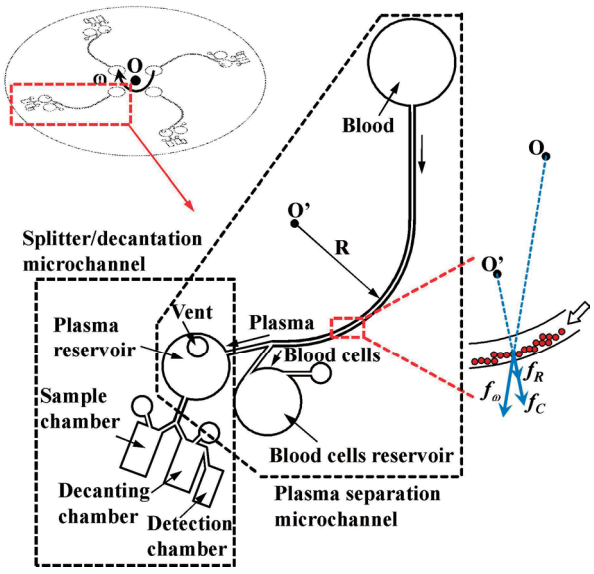

Fig. 7 Schematic illustrations of microchannel network configuration on proposed CD-type microfluidic platform [46].

In the straight region of the separation network, the Coriolis force is the only force acting on the sample. As a result, only a

minor separation of the plasma and blood cells occurs. However, in the curved region of the network, the sample is subjected to all three body forces, and the blood cells are driven toward the outer wall of the microchannel as a result of their greater density. Thus, on reaching the bifurcation point at the end of the curved channel, the blood cells flow into the blood cell reservoir, while the plasma continues in the downstream direction. According to the authors, the plasma within the whole blood sample was separated from the cells within 5-6 s under the rotation speed of 1800 rpm, and very few blood cells remained within the plasma as it flowed past the bifurcation point and entered the plasma reservoir.

T.-H. Kim *et al.* [47] studied further on the geometry effects of the microchannel on blood separation rate on the CD-type microfluidic platform. According to the authors, the plasma separation rate was enhanced significantly, as much as 8 times faster from whole blood by simply changing the channel geometry. As shown in Fig. 8, for the microchannel with narrower widths and larger tilt angles with respect to the radial direction, it is better to get higher separation rate. However, the channel depth or rotation direction has no effect on increasing the separation rate.

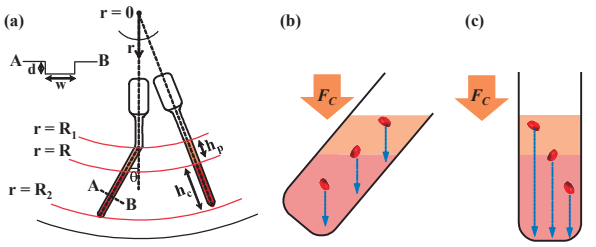

Fig. 8 Schematic diagram showing the blood cell sedimentation on a CD-type microfluidic platform (a). Blood separation in a tilted channel (b) and a straight channel (c). As the blue arrows indicate, the particle sedimentation distance is shorter in a slanted than a straight channel [47].

The authors use the Ponder-Nakamura-Kuroda (PNK) theory [44-45] to explain the enhancement of separation rate in the slanted microchannel, which is due to the increase in the surface area available for settling. For instance, the blood cells can only settle onto the bottom in a straight microchannel while the blood cells can also settle onto the upward-facing wall in the slanted microchannel. During the blood cells sedimentation process, the cells first approach the wall of an inclined wall and form concentrated slurry which is significantly heavier than the clear plasma and rapidly slides down toward the downstream of the microchannel.

A. Prabhakar *et al.* [48] presented a work in which a combination of effects such as Fahraeus effect, bifurcation law, cell-free region, centrifugal action and constriction-expansion was utilized together for separating plasma from human blood.

As shown in Fig. 9, the microfluidic design has on inlet microchannel (for blood inlet), connected to blood inlet reservoir and two outlet microchannels for plasma and blood flow connected to respective reservoirs. The blood outlet reservoir is named O and the two plasma reservoirs are named P1 and P2. According to the authors, the proposed design benefits of bifurcation law (via T shape of microchannel), aggregation (via suitable elevated dimension of microchannel), centrifugation (via bend shape of microchannel), constriction (via constricting the microchannel dimension in bend region) and expansion (via expanding the microchannel dimension suddenly after bend region). The experimental results show that almost 100% of separation efficiency has been achieved at moderate hematocrit contents of around 20%, and the separation efficiency for undiluted blood sample (hematocrit of 45%) is around 80%.

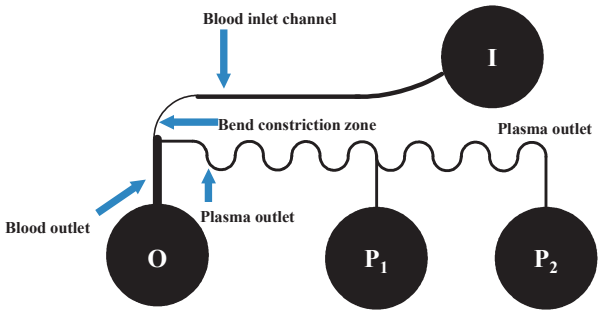

Fig. 9 Schematic diagram of blood plasma separation device [48].

5. Flow sequencing

Since the beginning of the research in the field of CD-type microfluidic platform, adjustment of flow sequencing using passive valves is the most widely used one introduced by Madou *et al.* [60] and Zoval *et al.* [61]. Passive valve is based on balancing the capillary force (due to the fluid interfacial tension) and the centrifugal force (due to the rotation of the device). When the centrifugal force exceeds the capillary force, liquid starts moving and is released from one reservoir to another. Proper distribution of reservoirs on the device with a proper design of microchannel network could allow for controlled flow sequencing. The rotation frequency at which the centrifugal force overcomes the capillary force to open the passive valve is defined as the burst frequency, and precise control of burst frequency allows for a synchronized flow sequencing of solutions for carrying out complex assay processes on the CD-type microfluidic platform.

Several mathematical models for describing passive valves have already been published in last decades, from 1 D model to more complex 2D and 3D models [62-64]. Based on the development in the theoretical aspect, various approaches for adjusting the flow sequence are proposed by the researchers in the last few years [65-72]. L. Clime *et al.* [67] combined a regulated pressure pump with a programmable electromechanical valving system to control the microfluidic flow sequence. L.-L. Fan *et al.* [70] designed a microchannel with asymmetric sharp corners to realize the combination of inertial lift force effect and centrifugal force effect to realize a single and highly focused particle streams on the CD-type microfluidic platform. And M. Kitsara *et al.* [71] worked from the aspect of surface modification, by spin-coating the hydrophilic polymeric film, to enhance the centrifugal flow control by using the serial siphoning structure.

T. H. G. Thio *et al.* [65] recently published a study of theoretical development and critical analysis of burst frequency equations for passive valves on the CD-type microfluidic platforms. Compared with the previous study, the authors divided the meniscus propagation in hydrophilic valve into four distinct phases: capillary flow is stopped at the channel opening (1), the fluid movement is resumed under the increased force (2), the concave meniscus becomes convex (3), and then it

expands and finally bursts (4). A more accurate version of the burst frequency equation for the capillary valves is proposed, and the modified equations are used to evaluate the effects of various CD design parameters such as the hydraulic diameter, the height to width aspect ratio and the opening wedge angle of the channel on the burst pressure.

Y. Ukita *et al.* [66] proposed a very interesting work on the adjustment of the flow sequencing by using a so-called water-clock valve under the constant rotation speed. As shown in Fig. 10, a vent was connected to the water clock, and opposite the vent hole, a waste reservoir with its own vent hole was connected to the water clock through a microchannel. The four reservoirs were paralleled connected to the water clock with microchannels, respectively.

Under the constant rotation speed, the liquid in the water clock (working fluid) flowed out from the water clock by the centrifugal force. Four sample reservoirs were connected to the water clock through four parallel microchannels. The air supply to the sample reservoir was therefore blocked by the working fluid in the water clock. When the working liquid level was decreasing due to the flow out of the solution, the blocking to the air supply to the four sample reservoirs was sequentially released, so that the solutions in the four sample reservoirs could flow out sequentially into the corresponding waste reservoir. According to the authors, the time trigger for the solutions in the four sample reservoirs was highly reproducible, and a typical error of less than 3% was achieved. The authors' work gives another aspect of idea to adjust the flow sequencing on the CD-type microfluidic platform, and this simple configuration of water-clock-based flow sequencing is also very convenient to cooperate with other downstream unit operations to realize the automation and integration of bioanalysis applications on the device.

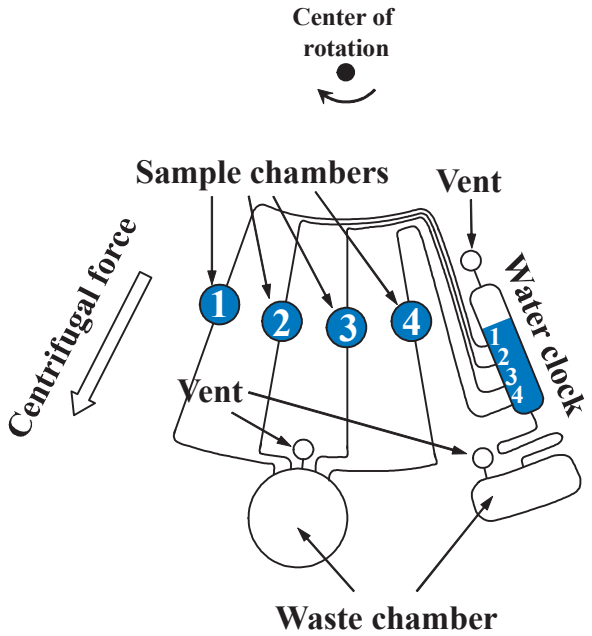

Fig. 10 Schematic illustration of the water-clock-based flow sequencer in the initial state of the experiment [66].

6. Conclusion

In this review, we introduce the recent development of the fundamental functions of compact disc (CD)-type microfluidic platform, in the aspects of valving, mixing, separation and the adjustment of flow sequencing, which are all very important and essential to realize the automation and integration of bioanalysis processes on the device. In last few years (2012-2015), many researchers paid attentions to the field of CD-type microfluidic platform, and proposed various ideas to improve to equip the functions to this CD-sized device greatly. In this review, we summarize the recent work on the fundamental functions of CD-type microfluidic platform, and hopefully this review can help the readers to have an overall motivation for further development in this research field.

The CD-type microfluidic platform is still a young technique, and many aspects in this filed are still not mature and well developed, compared with the traditionally analytical methods such as chromatography, mass spectrometry, electrophoresis and so on. However, the CD-type microfluidic platform stands for the trend of the development in the analytical methods, which is miniaturization, integration, automation, low-cost, low consumption of reagents and so on. Based on the great contributions by many researchers, the CD-type microfluidic platform has the potential to be developed into a powerful tool in the analytical chemistry field in the future.

References

[1] C. T. Schembri, T. L. Burd, A. R. Kopf-Sill, L. R. Shea, B. Braynin, *J. Autom. Chem.* **17**, 99 (1995).
[2] M. J. Madou, J. Florkey, *Chem. Rev.* **100**, 2679 (2000).
[3] I. H. A. Badr, R. D. Johnson, M. J. Madou, L. G. Bachas, *Anal. Chem.* **74**, 5569 (2002).
[4] L. G. Puckett, E. Dikici, S. Lai, M. J. Madou, L. G. Bachas, S. Daunert, *Anal. Chem.* **76**, 7263 (2004).
[5] S. Lai, S. Wang, J. Luo, L. J. Lee, S.-T. Yang, M. J. Madou, *Anal. Chem.* **76**, 1832 (2004).
[6] D. C. Duffy, H. L. Gillis, J. Lin, N. F. Sheppard, Jr., G. J. Kellogg, *Anal. Chem.* **71**, 4669 (1999).
[7] B. Zhao, J. S. Moore, D. J. Beebe, *Anal. Chem.* **74**, 4259 (2002).
[8] J. Lee, H. Moon, J. Fowler, T. Schoellhammer, C.-J. Kim, *Sens. Actuators, A* **95**, 259 (2002).
[9] T.-S. Leu, P.-Y. Chang, *Sens. Actuators, A* **115**, 508 (2004).
[10] J. Kim, H. Kido, R. H. Rangel, M. J. Madou, *Sens. Actuators, B* **128**, 613 (2008).
[11] W. Al-Faqheri, F. Ibrahim, T. H. G. Thio, J. Moebius, K. Joseph, H. Arof, M. J. Madou, *PLoS ONE* 8(3): e58523. doi:10.1371/journal.pone.0058523 (2013).
[12] A. Kazemzadeh, P. Ganesan, F. Ibrahim, M. M. Aeinehvand, L. Kulinsky, M. J. Madou, *Sens. Actuators, B* **204**, 149 (2014).
[13] L. Swayne, A. Kazarine, E. J. Templeton, E. D. Salin, *Talanta* **134**, 443 (2015).
[14] W. Al-Faqheri, F. Ibrahim, T. H. G. Thio, M. M. Aeinehvand, H. Arof, M. J. Madou, *Sens. Actuators, A* **222**, 245 (2015).
[15] Z. Cai, J. Xiang, B. Zhang, W. Wang, *Sens. Actuators, B* **206**, 22 (2015).
[16] Z. Cai, J. Xiang, W. Wang, *Sens. Actuators, B* **221**, 257 (2015).
[17] M. M. Aeinehvand, F. Ibrahim, S. W. Harun, A. Kazemzadeh, H. A. Rothan, R. Yusof, M. J. Madou, *Lab Chip* **15**, 3358 (2015).
[18] Y. Zhao, F. Schwemmer, S. Zehnle, F. V. Stetten, R.

Zengerle, N. Paust, *Lab Chip* **15**, 4133 (2015).
[19] D. J. Kinahan, S. M. Kearney, O. P. Faneuil, M. T. Glynn, N. Dimov, J. Ducrée, *RSC Adv.* **5**, 1818 (2015).
[20] R. Gorkin, C. E. Nwankire, J. Gaughran, X. Zhang, G. G. Donohoe, M. Rook, R. O'kennedy, J. Ducrée, *Lab Chip* **12**, 2894 (2012).
[21] L. X. Kong, K. Parate, K. Abi-Samra, M. J. Madou, *Microfluid. Nanofluid.* **18**, 1031 (2015).
[22] W. Al-Faqheri, F. Ibrahim, T. H. G. Thio, N. Bahari, H. Arof, H. A. Rothan, R. Yusof, M. J. Madou, *Sensors* **15**, 4658 (2015).
[23] F. Schwemmer, S. Zehnle, D. Mark, F. V. Stetten, R. Zengerle, N. Paust, *Lab Chip* **15**, 1545 (2015).
[24] Y. Kim, S.-N. Jeong, B. Kim, D.-P. Kim, Y.-K. Cho, *Anal. Chem.* **87**, 7865 (2015).
[25] A. Kazemzadeh, P. Ganesan, F. Ibrahim, L. Kulinsky, M. J. Madou, *RSC Adv.* **5**, 8669 (2015).
[26] M.-S. Choi, J.-C. Yoo, *Appl. Biochem. Biotechnol.* **175**, 3778 (2015).
[27] D. J. Kinahan, S. M. Kearney, N. Dimov, M. T. Glynn, J. Ducrée, *Lab Chip* **14**, 2249 (2014).
[28] Y. Deng, J. Fan, S. Zhou, T. Zhou, J. Wu, Y. Li, Z. Liu, M. Xuan, Y. Wua, *Biomicrofluid.* **8**, 024101 (2014).
[29] X. Du, L. Guo, *Adv. Mater. Res.* **631**, 858 (2013).
[30] T. Kawai, N. Naruishi, H. Nagai, Y. Tanaka, Y. Hagihara, Y. Yoshida, *Anal. Chem.* **85**, 6587 (2013).
[31] M. Amasia, M. Cozzens, M. J. Madou, *Sens. Actuators, B* **161**, 1191 (2012).
[32] R. Gorkin, S. Soroori, W. Southard, L. Clime, T. Veres, H. Kido, L. Kulinsky, M. J. Madou, *Microfluid. Nanofluid.* **12**, 345 (2012).
[33] J. M. Ottino, S. Wiggins, *Philos. Trans. Roy. Soc. Lond. A* **362**, 923 (2004).
[34] T. G. Kang, M. K. Singh, T. H. Kwon, P. D. Anderson, *Microfluid. Nanofluid.* **4**, 589 (2008).
[35] R. Wang, J. Lin, H. Li, *Chaos Solution. Fract.* **33**, 1362 (2007).
[36] H. E. H. Meijer, M. K. Singh, T. G. Kang, J. M. J. den Toonder, P. D. Anderson, *Macromol. Symp.* **279**, 201 (2009).
[37] M. Grumann, A. Geipel, L. Riegger, R. Zengerle, J. Ducrée, *Lab Chip* **5**, 560 (2005).
[38] Y. Ren, W. W.-F. Leung, *Chem. Eng. J.* **215**, 561 (2013).
[39] J.-N. Kuo, L.-R. Jiang, *Microsyst. Technol.* **20**, 91 (2014).
[40] W. W.-F. Leung, Y. Ren, *Int. J. Heat Mass Tran.* **64**, 457 (2013).
[41] M. C. R. Kong, E. D. Salin, *Microfluid. Nanofluid.* **13**, 519 (2012).
[42] M. Toner, D. Irimia, *Annu. Rev. Biomed. Eng.* **7**, 77 (2005).
[43] P. Yager, T. Edwards, E. Fu, K. Helton, K. Nelson, M. R. Tam, B. H. Weigl, *Nature* **442**, 412 (2006).
[44] E. Ponder, *Exp. Physiol.* **15**, 235 (1925).
[45] H. Nakamura, K. K. Kuroda, *J. Med.* **8**, 256 (1937).
[46] J.-N. Kuo, X.-F. Chen, *Microsyst. Technol.* **21**, 2485 (2015).
[47] T.-H. Kim, H. Hwang, R. Gorkin, M. J. Madou, Y.-K. Cho, *Sens. Actuators, B* **178**, 648 (2013).
[48] A. Prabhakar, Y V B. V. Kumar, S. Tripathi, A. Agrawal, *Microfluid. Nanofluid.* **18**, 995 (2015).
[49] T. Morijiri, M. Yamada, T. Hikida, M. Seki, *Microfluid. Nanofluid.* **14**, 1049 (2013).
[50] H. J. Jeon, D. I. Kim, M. J. Kim, X. D. Nguyen, D. H. Park, J. S. Go, *J. Micromech. Microeng.* **25**, 114001 (2015).
[51] M. T. Glynn, D. Kirby, D. Chung, D. J. Kinahan, G. Kijanka, J. Ducrée, *J. Lab. Autom.* **19**, 285 (2014).
[52] D. Kirby, J. Siegrist, G. Kijanka, L. Zavattoni, O. Sheils, J. O'Leary, R. Burger, J. Ducrée, *Microfluid. Nanofluid.* **13**, 899 (2012).
[53] E. J. Templeton, E. D. Salin, *Microfluid. Nanofluid.* **17**, 245 (2014).
[54] J. C. Yeo, Z. Wang, C. T. Lim, *Biomicrofluid.* **9**, 054114 (2015).
[55] J. Zhang, X. Wei, X. Xue, Z. Jiang, *J. Nanosci. Nanotechnol.* **14**, 7419 (2014).
[56] P. Arosio, T. Müller, L. Mahadevan, T. P. J. Knowles, *Nano Letters* **14**, 2365 (2014).
[57] D. Kirby, M. T. Glynn, G. Kijanka, J. Ducrée, *Cytom. Part A* **87**, 74 (2015).
[58] R. Burger, N. Reis, J. G. Da Fonseca, J. Ducrée, *J. Micromech. Microeng.* **23**, 035035 (2013).
[59] D. J. Kinahan, S. M. Kearney, M. T. Glynn, J. Ducrée, *Sens. Actuators, A* **215**, 71 (2014).
[60] M. J. Madou, J. V. Zoval, G. Jia, H. Kido, J. Kim, N. Kim, *Annu. Rev. Biomed. Eng.* **8**, 601 (2006).
[61] J. V. Zoval, M. J. Madou, *Proc. IEEE* 140 (2004).
[62] J. M. Chen, P. C. Huang, M. G. Lin, *Microfluid. Nanofluid.* **4**, 427 (2008).
[63] J. Kim, H. Kido, R. H. Rangel, M. J. Madou, *Sens. Actuators, B* **128**, 613 (2008).
[64] P. F. Man, C. H. Mastrangelo, M. A. Burns, D. T. Burke, *Proc. IEEE* 45 (1998).
[65] T. H. G. Thio, S. Soroori. F. Ibrahim, W. Al-Faqheri, N. Soin, L. Kulinsky, M. J. Madou, *Med. Biol. Eng. Comput.* **51**, 525 (2013).
[66] Y. Ukita, Y. Takamura, Y. Utsumi, *Sens. Actuators, B* **220**, 180 (2015).
[67] L. Clime, D. Brassard, M. Geissler, T. Veres, *Lab Chip* **15**, 2400 (2015).
[68] S. Z. Andreasen, D. Kwasny, L. Amato, A. L. Brøgger, F. G. Bosco, K. B. Andersen, W. E. Svendsen, A. Boisen, *RSC Adv.* **5**, 17187 (2015).
[69] A. Kezarine, E. D. Salin, *Lab Chip* **14**, 3572 (2014).
[70] L.-L. Fan, Y. Han, X.-K. He, L. Zhao, J. Zhe, *Microfluid. Nanofluid.* **17**, 639 (2014).
[71] M. Kitsara, C. E. Nwankire, L. Walsh, G. Hughes, M. Somers, D. Kurzbuch, X. Zhang, G. G. Donohoe, R. O'kennedy, J. Ducrée, *Microfluid. Nanofluid.* **16**, 691 (2014).
[72] H. C. Chang, Y. H. Chen, S. L. Lin, S. S. Hung, *Appl. Mech. Mater.* **397**, 1733 (2013).

(Received January 11, 2016)

(Accepted January 22, 2016)